JOURNAL OF MATERIALS SCIENCE **36** (2001) 1569–1575

Eutectic reaction and microstructural characteristics of Al (Li)-Mg_2Si alloys

S.-P. LI*, S.-X. ZHAO, M.-X. PAN†, D.-Q. ZHAO, X.-C. CHEN
Institute of Physics, Academia Sinica, Beijing 100080, People's Republic of China
E-mail: panmx@aphy.iphy.ac.cn

O. M. BARABASH
Institute of Metal Physics, Kiev 252142, Ukraine

Thermal analysis, directional solidification and metallographic techniques were applied to investigate the pseudobinary eutectic reaction process and the microstructural characteristics of Al(Li)-Mg_2Si alloys. It was demonstrated that the eutectic reaction curve for $L \Leftrightarrow Al(Li) + Mg_2Si$ in the Al(Li)-Mg-Si system moves to the Al-rich corner with the increase of Li additions. The pseudobinary eutectic point with the highest melting temperature and null temperature range of solidification (ΔT) and the ternary eutectic point for $L \Leftrightarrow Al(Li) + Mg_2Si + Si$ all move towards the Si-rich direction. Li additions widen the range of yielding binary eutectic of Al(Li)-Mg_2Si and depress the appearing of ternary eutectic efficiently. Al(Li)-Mg_2Si eutectic alloys have the best aligned structure when the directional solidification occurs with a $\Delta T = 0$. The Mg_2Si phase has a diversity of morphologies such as rod-like, crossed and rooftop-like. These various morphologies has the same preferred growth direction, i.e. [100]. © *2001 Kluwer Academic Publishers*

1. Introduction

It is well known that aluminum-lithium alloys are suitable for weight-critical applications. Lithium additions to aluminum give the greatest reduction in density and increase in elastic modulus per wt % of all known alloying elements. Lithium is one of the few elements with substantial solubility in solid aluminum (4.2 wt % in binary aluminum-lithium alloy) [1]. The intermetallic compound Mg_2Si also becomes increasingly attractive as a reinforcing phase in Al-matrix alloys and composites because of its high melting point, low density and high strength [2, 3].

A pseudobinary eutectic reaction exists between phases Al and Mg_2Si with volume fraction of 14.2 at% Mg_2Si phase, which satisfies the regularity of the normal commercial nonfaceted-faceted eutectic alloys. Studies on the eutectic reaction and microstructural characteristics of the Al-Mg_2Si eutectic have been reported [4, 5], which declared its possibility of being developed as a potential directionally solidified eutectic composite. Since Li has little reactivity with compound Mg_2Si [6], mechanical properties of the Al-Mg_2Si eutectic could be improved further when the Al matrix is strengthened by Li addition. However, the composition of the eutectic reaction in the phase diagram changes and its morphology has different characteristics in this case. In this work, we present the resuit of a study on $L \Leftrightarrow Al(Li) + Mg_2Si$ eutectic reaction with different Li additions by thermal analyses and metallographic techniques. The eutectic points where $\Delta T = 0$ will be traced to optimize the solidification structures.

2. Experimental procedure

Alloy ingots were prepared by melting pure Al, Mg and Si with purity above 99.99% in an electric resistance furnace under the protection of LiCl flux. Smith's thermal analyses method [7] which is sensitive to the range of the phase transition was applied to measure the value of ΔT under the protection of high-purity helium. Fig. 1 shows a schematic thermal analyses curve with this method. The whole experimental data (T, ΔT) were taken from the heating curve, and the data taken from the cooling curve are only for reference.

Directional solidification was performed by an electron-beam zone melting technique using a ring electron gun as heater working in a vacuum of $\sim 10^{-3}$ Pa which provides a comparatively narrow melting zone and a rather constant temperature gradient. Specimens for directional solidification were placed in a graphite tube with a inner size of $\phi 8 \times 110$ mm and were naturally cooled. The temperature gradient ahead of the solid-liquid interface in the melt was measured to be 6.3×10^3 °C/m.

Investigation on the microstructures was carried out on Neophot-21 optical microscope and S-4200 scanning electron microscope, and philips-420 transmission electron microscope was used to analyze orientation of the phases.

* *Present Address*: PCS Group, Cavendish Laboratory, Maldingey Road, Cambridge CB3 0HE, UK.

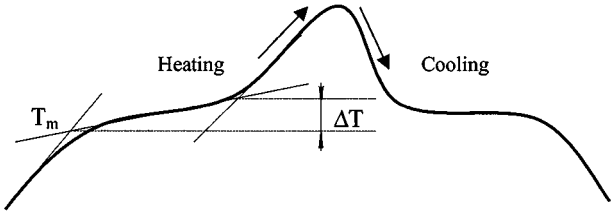

Figure 1 Schematic diagram of process for thermal analyses.

3. Results

3.1. Thermal analyses for the eutectic curve

Series of Al-Mg_2Si alloys with nil, 1.0 wt %, 2.0 wt % and 3.0 wt % Li additions were prepared, and then thermal analyses and metallographic analyses were carried out upon these alloys. Based on the thermal and metallographic analyses results the effect of Li additions on the pseudobinary eutectic reaction is illustrated in the phase diagrams of Ai-rich corner in the Al-Mg-Si system. As can be seen in Fig. 2. The eutectic reaction curve C_i ($i = 0, 1, 2, 3$, which corresponds to nil, 1.0 wt%, 2.0 wt% and 3.0 wt% Li additions, respectively) has the following variation with the increase of Li additions:

(1) The eutectic curve C_i moves towards the Al-rich corner;

(2) The eutectic point e_i at which $\Delta T = 0$ moves towards the Si-rich direction;

(3) The ternary eutectic point e_i^t for $L \Leftrightarrow Al(Li) + Mg_2Si + Si$ moves towards the Si-rich direction;

(4) Li additions cause widening of the range between points M_i and N_i which correspond to two critical

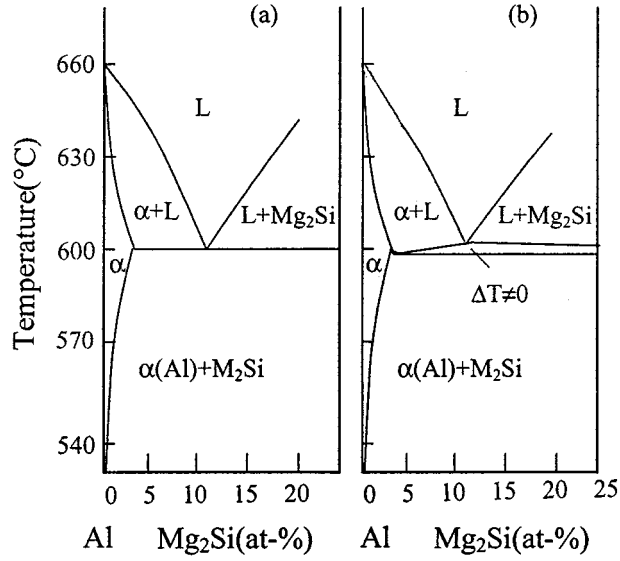

Figure 3 Schematic diagrams of pseudobinary eutectic reaction along A-B and Al + Mg_2Si lines which is shown in Fig. 2a. The eutectic reaction defined by A-B line which passes point e_0 has a null temperature range of solidification ($\Delta T = 0$) as showing in Fig. 3a. Such diagrams, the only Al(Li)-Mg_2Si pseudobinary eutectic reaction with $\Delta T = 0$ for each Li addition, also can be obtained from Fig. 2b–d.

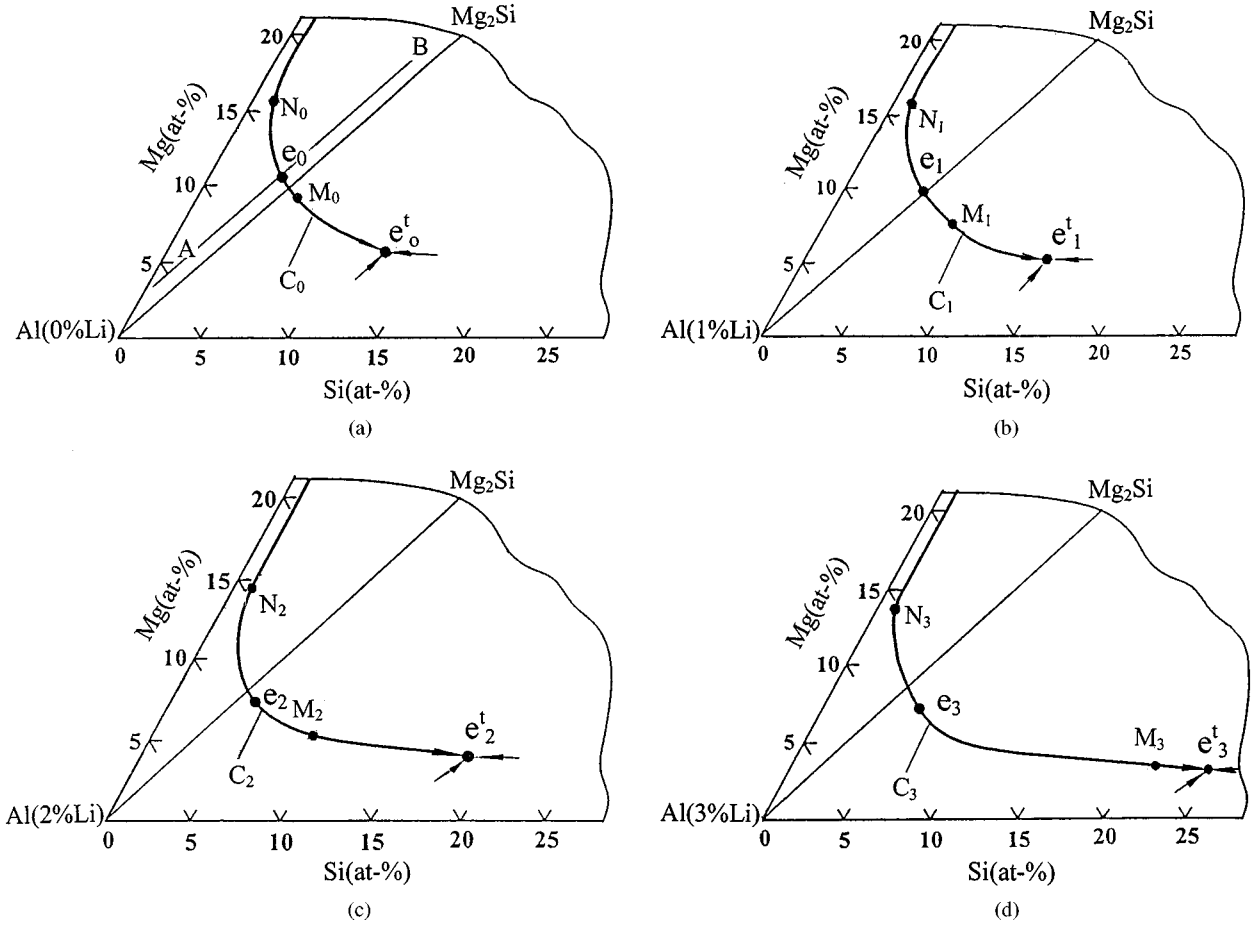

Figure 2 Projection of the eutectic curves where the two liquidus surfaces of primary Al(Li) and Mg_2Si are intersected in Al(Li)-Mg-Si system showing the effect of Li additions on the pseudobinary eutectic; (a) nil Li; (b) 1.0 wt%Li; (c) 2.0 wt%Li; (d) 3.0 wt%Li.

points where $L \Leftrightarrow Al(Li) + Mg_2Si + Si$ and $L \Leftrightarrow Al(Li) + Mg_2Si + Mg_5Al_8$ ternary eutectic transition occur, respectively. Binary $Al(Li) + Mg_2Si$ eutectic structure without Al(Li) or Mg_2Si dendrites could be obtained if the composition is selected between points M_i and N_i along the eutectic reaction curve.

Among these factors, (2), (3) and (4) are of high potential application value. Moving of points e_i and e_i^t in the direction of increasing of Si content and decreasing of Mg content satisfies the requirement on industrial alloys. Widening of the gap between M_i and N_i in Fig. 2 caused by additions of Li will suppress the appearance of ternary eutectics in a wider composition range. Ternary eutectic that has a lower melting temperature in an alloy tends to concentrate at the grain boundary in a casting at the latest stage of solidification, which will impair its mechanical properties at medium and high temperature. Fig. 3 presents two schematic diagrams of pseudobinary eutectic reaction along A-B and Al+Mg_2Si lines in Fig. 2a. It is clear that the eutectic reaction defined by A-B line which passes point e_0 has a null temperature range of solidification($\Delta T = 0$).

In order to clarify the eutectic solidification feature in Al(Li)+Mg_2Si system we present the melting temperature T_m and temperature range of solidification ΔT for each component on the eutectic curves C_i in Fig. 4. For a simple description of this relation in two dimensional coordinate, we take the composition ratio of Mg and Si (C_{Mg}/C_{Si}) of each point on the C_i curves to be the content axis. It can be seen clearly from Fig. 4 that for each Li addition, there exists a point e_i on the eutectic reaction curve where $\Delta T = 0$, and the melting temperature T_m is the highest. When the composition of the alloy deviates from point e_i, its ΔT does not equal zero and the melting temperature decreases, which is unfavorable to its solidification structure and the resultant properties. For alloys with $\Delta T = 0$ there

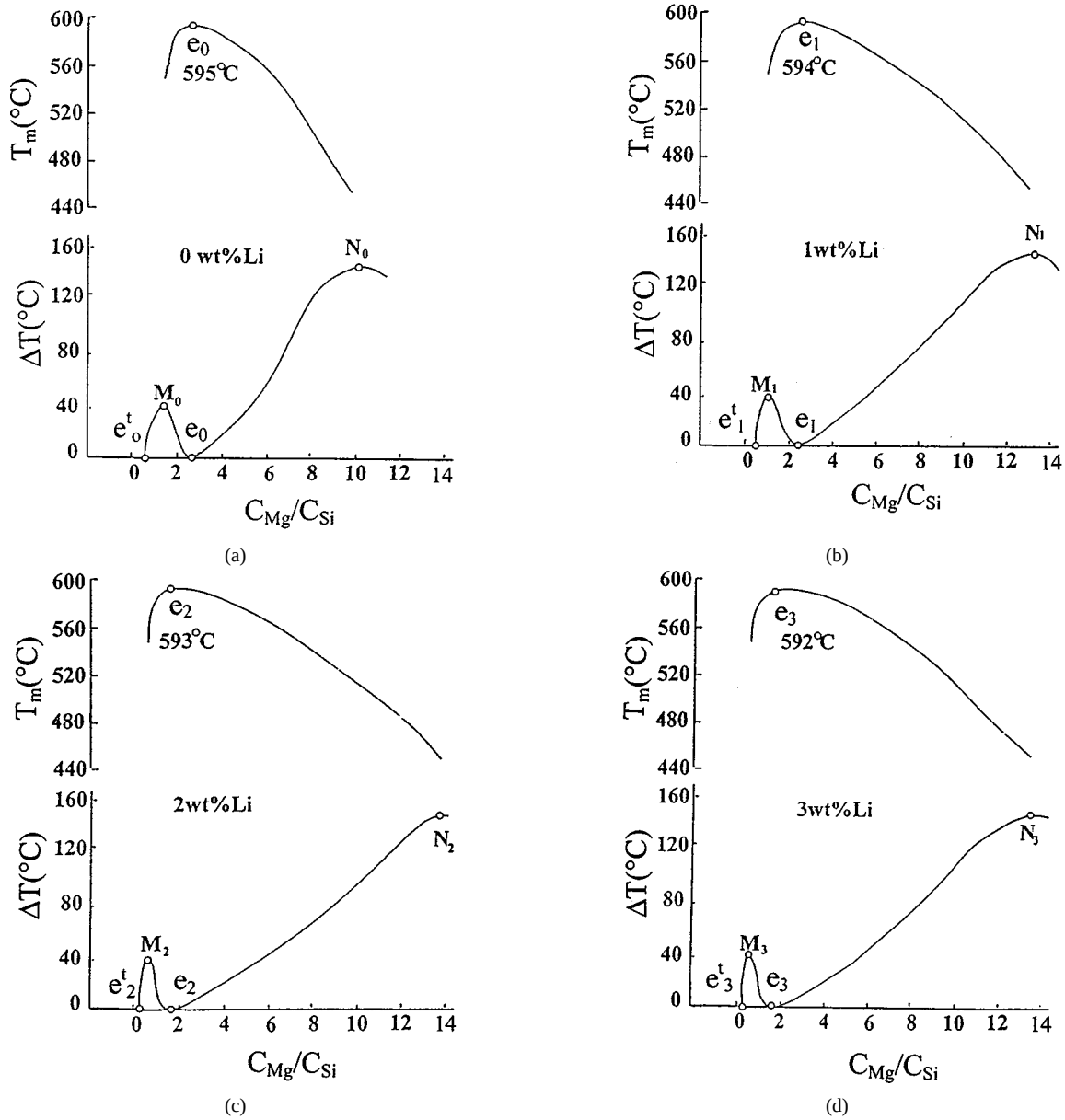

Figure 4 Measurement results on the melting temperature T_m and the temperature range of solidification ΔT of various points on the eutectic curves for different Li additions; (a) nil Li; (b) 1.0 wt%Li; (c) 2.0 wt%Li; (d) 3.0 wt%Li. The composition ratio of Mg and Si is taken as the content axis. Each C_{Mg}/C_{Si} value corresponds to one composition on the eutectic cures C_i.

is no primary phase formed and the resultant structure is uniform. This is of considerable importance, especially in the case of preparing a directional solidified eutectic composite material of this system. Only when the solidification is carried out at a constant temperature the solid-liquid interface have the highest stability during directional solidification to result in a well aligned composite structure of this eutectic readily. Alloys with composition on points M_i and N_i have the largest temperature range of solidification. Point e_i^t is the ternary eutectic point where the solidification range equals zero too. The melting temperature of the eutectic alloys decreases with the increase of Li additions, but the variation is small.

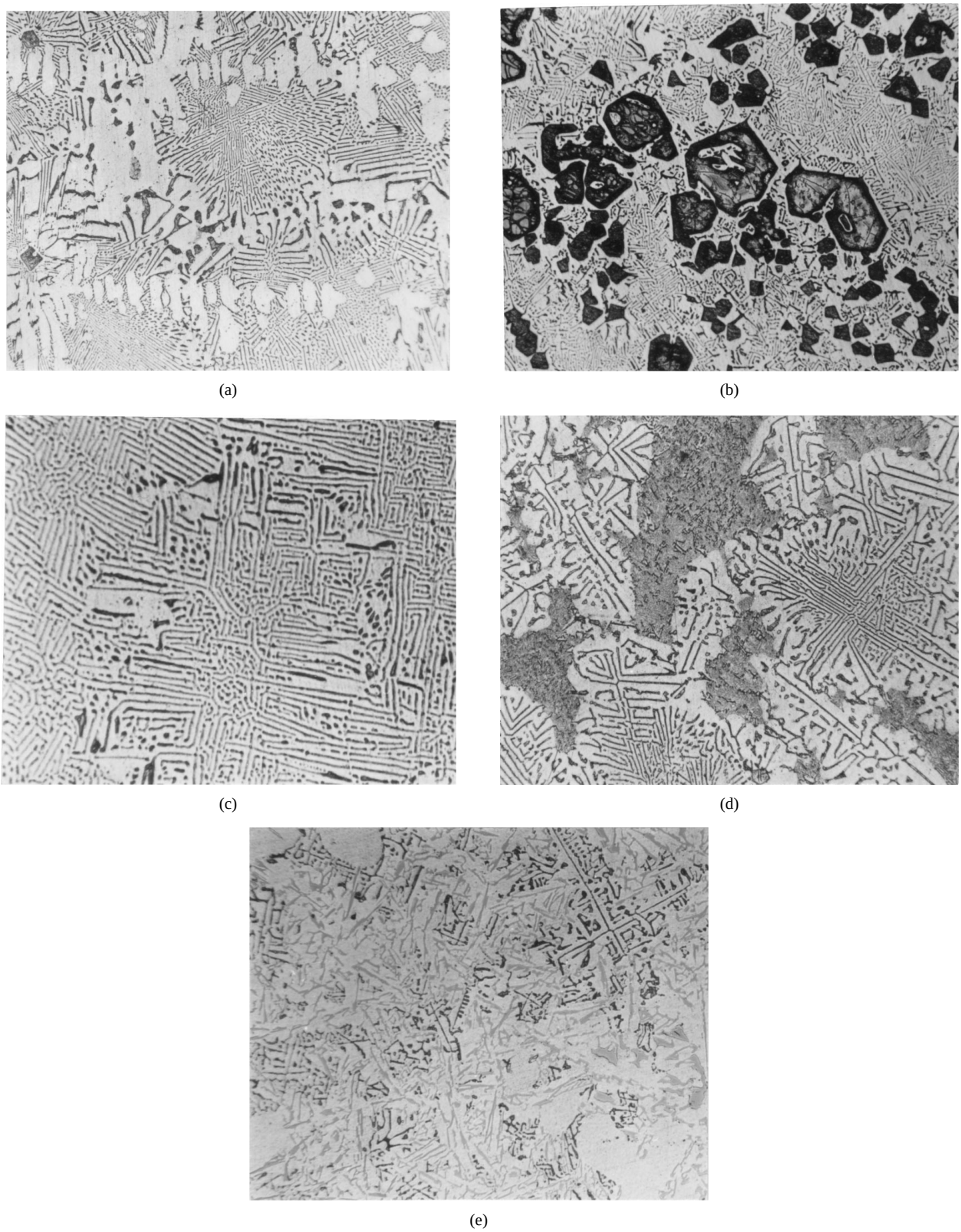

Figure 5 Several typical freely solidified structures of Al(Li)-Mg_2Si alloys; (a) hypoeutectic; (b) hypereutectic; (c) binary eutectic; (d) containing little ternary eutectic; (e) ternary eutectic.

3.2. Microstructural characteristics

Various structures can be obtained when the composition of the alloys falls in different areas in Fig. 2. A mixed structure of the eutectic and the dendritic Al(Li) or Mg_2Si as shown in Fig. 5a and 5b will be produced if composition of the alloys is below or above the eutectic curve C_i, respectively. A perfect binary eutectic structure as shown in Fig. 5c appears if the composition is selected between M_i and N_i points on the eutectic curve C_i. A three-phases structure of $Al(Li) + Mg_2Si + Si$ starts to appear together with the $Al(Li) + Mg_2Si$ binary eutectic structure as shown in Fig. 5d when the alloy

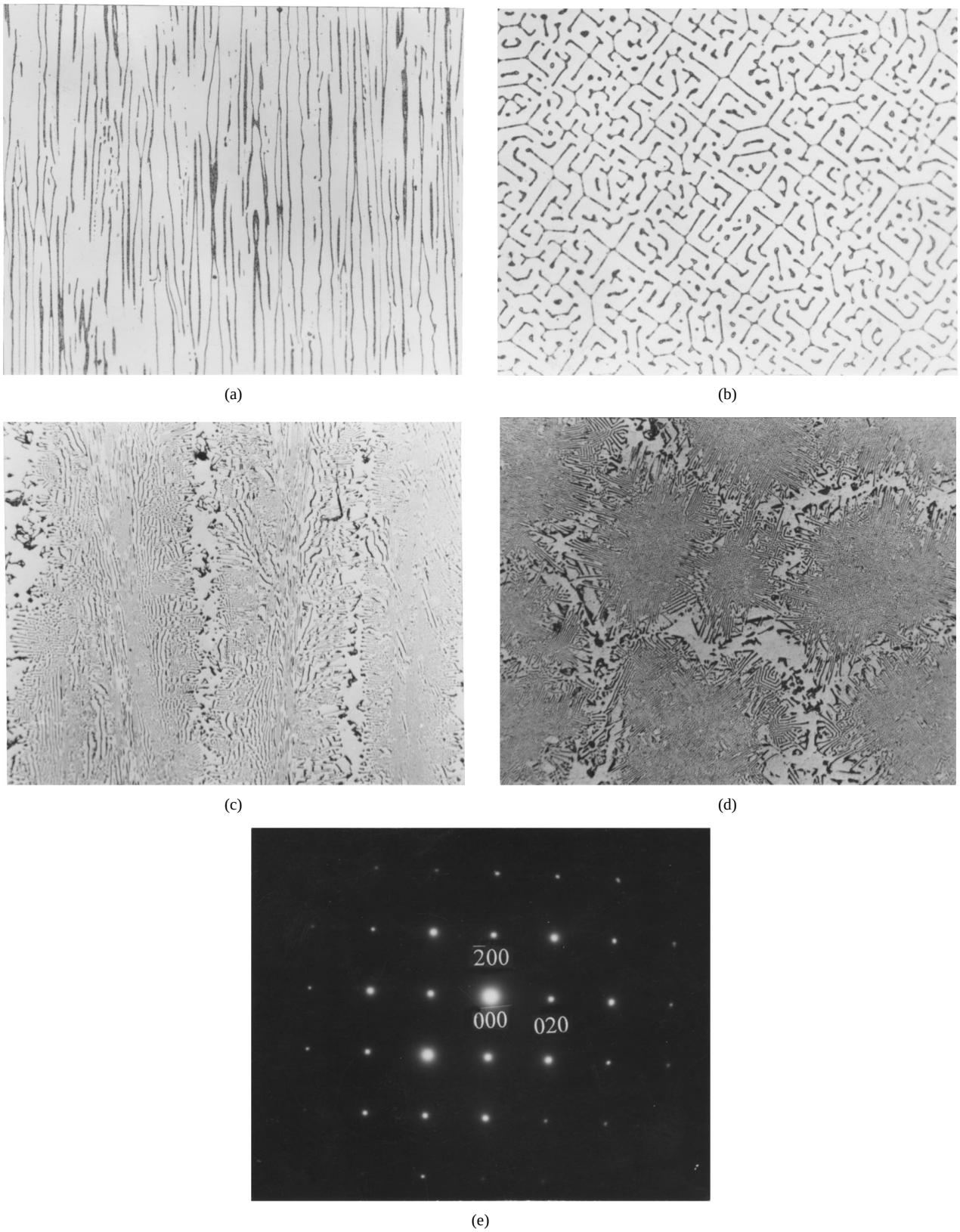

Figure 6 Typical structures of directionally solidified Al(Li)-Mg_2Si alloys and the electron diffraction analyses of phase Mg_2Si; (a) Well-aligned longitudinal structures; (b) Well-aligned transversal structures; (c) cellular longitudinal structures; (d) cellular transversal structures; (e) electron diffraction analyses of phase Mg_2Si of various morphologies in (b).

composition is on the Si-rich side of point M_i along the eutectic curve C_i. The structure consists of ternary eutectic, $Al(Li) + Mg_2Si + Si$, as shown in Fig. 5e when the alloy composition is at point e_i^t. Analogously, similar analyses can be made upon alloys to the Mg-rich direction, and the difference is that the ternary eutectic is that of $Al(Li) + Mg_2Si + Mg_5Al_8$. Alloys of these compositions are of poor industrial application values due to excess Mg.

As shown in Fig. 4, alloys with composition e_i are of high importance because only on these points $\Delta T = 0$, and the resultant eutectic structure is highly uniform. This is critical to the preparation of the directionally cast or directionally solidified composite materials since a stable solid-liquid interface and a highly aligned alloy structure during directional solidification can be achieved only when ΔT is small. A cellular or random structure instead of a well aligned structure will appear if ΔT is rather large. Fig. 6 illustrates the longitudinal and transversal structures of well aligned and cellular eutectic $Al(Li) + Mg_2Si$ after directional solidification. As can be seen from Fig. 6b, The Mg_2Si phase has a diversity of morphologies such as rod-like, crossed and rooftop-like. However, these different morphologies have the same crystallization direction which has been demonstrated to be [100] by electron diffraction analyses in this work (Fig. 6e).

4. Discussion

Shift of the binary eutectic curve to the Al-rich corner and that of the eutectic point to the Si-rich direction caused by Li additions can be considered in terms of the changing of the liquidus surface as shown schematicly in Fig. 7. Element Li has little reactivity with phase Mg_2Si [6] and Li additions will depress the liquidus temperature for Al(Li) solid solution to be below the melting temperature of pure aluminum. It can be considered that position of the liquidus surface for phase Mg_2Si will not change with Li content but that for phase Al(Li) move downwards with the increase of Li content (Fig. 7a), which will lead to the moving of the pseudobinary eutectic curve C_i to the Al-rich corner. The eutectic temperature also decreases simultaneously with the increases of Li additions.

On an isothermal section of Al(Li)-Mg-Si system, points of the liquid surface for primary Al and Mg_2Si were represented by two separated parabolds (Fig. 7b). Both parabolds approach each other on a isothermal section as temperature decreases and meet at a point which defines the eutectic point e_i. The Li addition influences not only the position of the parabolds that causes the decrease of T_e temperature but also the shape of the parabolds. The Li addition can dramatically move the binary eutectic point of Al-Si to the Si-rich derection [8] which is caused by the modification of liquid surface for primary Al. A similar modification of liquid surface for primary Al is expected in Al-Si-Mg system with the addition of Li which causes the change from of C_i curves and shift of point e_i to Si-rich direction. A schematic description of influence of Li addition on the position of C_i curves and e_i point is presented in Fig. 7b.

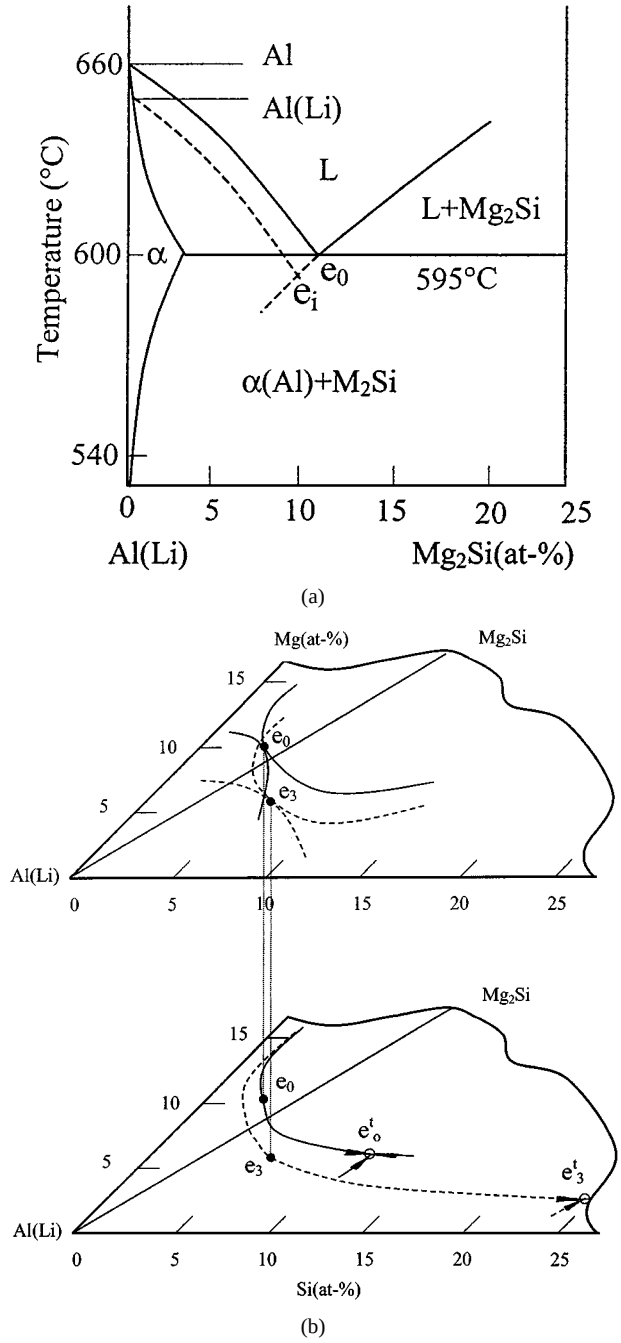

Figure 7 Schematic drawings of the effect of Li additions in Al(Li)-Mg_2Si system: (a) additions of Li shift the pseudobinary eutectic curve to the Al-rich direction and reduce the eutectic temperature. (b) Li additions change the form of C_i curves and move the e_i point towards the Si-rich direction through modification of liquid surface for primary Al: the upper drawing, scheme of the influence of Li on the point e_i where parabolds meet each other on an isothermal section; the lower drawing, scheme of the influence of Li on eutectic curve C obtained by reference of Fig. 2a and d. The solid curves—without Li additions; the dotted curves—with 3.0 wt%Li addition.

Diversification of the morphology of phase Mg_2Si after directional solidification can be interpreted in terms of the morphology of the primary crystal of Mg_2Si. Literature [9] demonstrated that in Al-Mg_2Si alloys there exist primary crystals of Mg_2Si having an octahedral shape as shown in Fig. 8a. Analyses manifest that the octahedral primary crystal of Mg_2Si is enclosed by {111} faces and its preferred growth direction is [100]. The preferred growth direction of directionally solidified Mg_2Si is the same as that of the primary crystal,

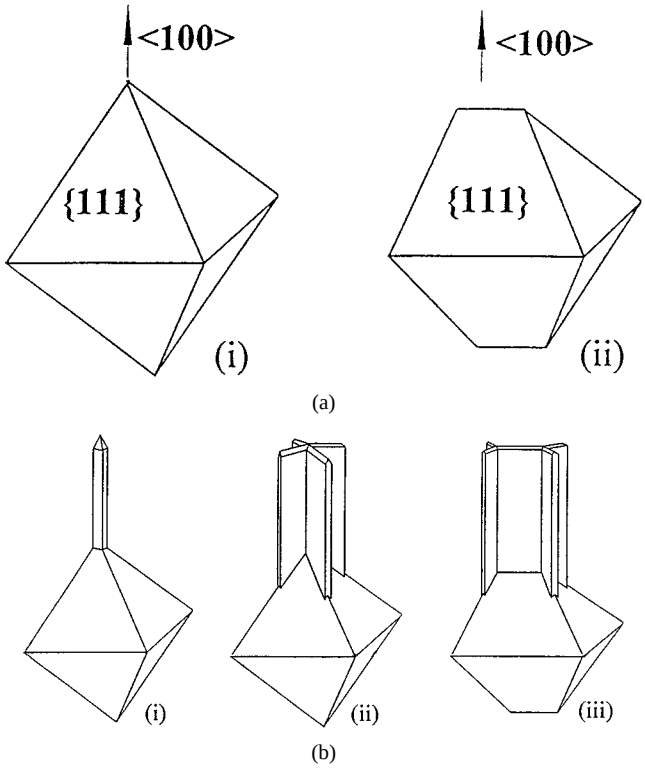

Figure 8 Schematic drawing of (a) primary crystal of Mg_2Si having an octahedral shape; (b) analyses on the forming mechanism of phase Mg_2Si of various morphologies.

which is defined by our electron diffraction analyses (Fig. 5e). At the early stage of solidification, eutectic Mg_2Si phase in ⟨100⟩ direction should be created in ⟨100⟩ direction of primary Mg_2Si crystals. The corners and edges of the primary crystal are the favourable sites for heat release and from where the eutectic Mg_2Si will arise preferably. When the eutectic Mg_2Si arises from the vertex of the corner of the regular octahedral primary crystal as shown in Fig. 8b i, it will posses a rod-like morphology. A crossed morphology as shown in Fig. 8b ii will be generated when the eutectic Mg_2Si phase arises from a vertex of a corner and the four neighboring edges of the regular octahedron. Analogously, a rooftop-like morphology of the eutectic Mg_2Si as shown in Fig.8b iii also arises from the ⟨100⟩ direction of the primary crystals. Certainly, the quantity and arrangement of these three morphologies as shown in Fig. 6b depend on the diffusion of the components and the interfacial energy between eutectic phases, which ensure that the inter-phase spacing λ is the same everywhere, because the solidification rate V and the eutectic spacing λ shall satisfy the equation, $\lambda^2 V = \text{const.}$ for a certain eutectic system [10].

5. Conclusions

(1) The eutectic reaction curve for the $L \Leftrightarrow Al(Li) + Mg_2Si$ in the Al(Li)-Mg-Si system moves to the Al-rich corner with the increase of Li additions. The pseudobinary eutectic point with the highest melting temperature and null temperature range of solidification, and the ternary eutectic point for $L \Leftrightarrow Al(Li) + Mg_2Si + Si$ both move to the Si-rich direction. Li additions widen the range of yielding the binary eutectic of $Al(Li) + Mg_2Si$ and depress the appearing of ternary eutectics.

(2) $Al(Li) + Mg_2Si$ eutectic alloys have the best directional solidification result when the temperature range solidification equals zero. Mg_2Si phase has a diversity of morphologies such as rod-like, crossed and rooftop-like, which has the same preferred growth direction i.e. [100].

References

1. E. J. LAVERNIA, T. S. SRIVATSAN and F. A. MOHAMED, *J. Mater. Sci.* **25** (1990) 1137.
2. M. MABUCHI, K. KUBOTA and K. HIGASHI, *Mater. Lett.* **19** (1994) 247.
3. M. RIFFEL and J. SCHILZ, *Scripta Meterialia* **32** (1995) 1951.
4. S.-P. LI, S.-X. ZHAO, M.-X. PAN and X.-C. CHEN, *Acta Metallurgica Sinica* **9** (1996) 306.
5. *Idem., ibid.* **9** (1996) 323.
6. L. F. MONDOLFO, "Aluminum Alloys, Structure and Properties" (Butterworths, London, 1976) p. 666
7. C. S. SMITH, *Trans. Am. Inst. Min. Met. Eng.* **137** (1940) 236.
8. M. D. HANNA and A. HELLAWELL, *Metallurgical Transactions A* **15A** (1984) 595.
9. E. E. SCHMID, K. VON OLDENBURG and G. FROMMEYER, *Z. Metallkde* **81** (1990) 809.
10. K. A. JACKSON and J. D. HUNT, *Trans. AIME* **236** (1966) 1129.

Received 18 December 1996
and accepted 10 February 2000